Cell, Vol. 115, 83–95, October 3, 2003, Copyright ©2003 by Cell Press

The Molecular Basis for Phosphodependent Substrate Targeting and Regulation of Plks by the Polo-Box Domain

Andrew E.H. Elia,[1,3,4] Peter Rellos,[2,4] Lesley F. Haire,[2] Jerry W. Chao,[1] Frank J. Ivins,[2] Katja Hoepker,[1] Duaa Mohammad,[1] Lewis C. Cantley,[3] Stephen J. Smerdon,[2,*] and Michael B. Yaffe[1,*]

[1]Center for Cancer Research
Department of Biology
Massachusetts Institute of Technology
Cambridge, Massachusetts 02139

[2]National Institute for Medical Research
Division of Protein Structure
London, NW7 1AA
United Kingdom

[3]Division of Signal Transduction
Department of Cell Biology
Beth Israel Deaconess Hospital
Harvard Medical School
Boston, Massachusetts 02215

Summary

Polo-like kinases (Plks) perform crucial functions in cell-cycle progression and multiple stages of mitosis. Plks are characterized by a C-terminal noncatalytic region containing two tandem Polo boxes, termed the Polo-box domain (PBD), which has recently been implicated in phosphodependent substrate targeting. We show that the PBDs of human, *Xenopus*, and yeast Plks all recognize similar phosphoserine/threonine-containing motifs. The 1.9 Å X-ray structure of a human Plk1 PBD-phosphopeptide complex shows that the Polo boxes each comprise $\beta_6\alpha$ structures that associate to form a 12-stranded β sandwich domain. The phosphopeptide binds along a conserved, positively charged cleft located at the edge of the Polo-box interface. Mutations that specifically disrupt phosphodependent interactions abolish cell-cycle-dependent localization and provide compelling phenotypic evidence that PBD-phospholigand binding is necessary for proper mitotic progression. In addition, phosphopeptide binding to the PBD stimulates kinase activity in full-length Plk1, suggesting a conformational switching mechanism for Plk regulation and a dual functionality for the PBD.

Introduction

Cyclin-dependent kinases (Cdks) have long been considered the master regulators of the cell cycle, but an increasing number of diverse protein kinases are now emerging as critical components of cell-cycle progression. Among these are members of the Polo-like kinase family (Plks) that play key roles during all stages of mitosis and in the cell cycle checkpoint response to genotoxic stress (Nigg, 1998; Glover et al., 1998). Many protein kinases involved in cell-cycle control function, in part, by generating phosphoserine/threonine-containing sequence motifs in their substrates that are subsequently recognized by phosphoserine/threonine binding proteins. These include the WW and proline isomerase domain of Pin1 that regulates mitotic progression, 14-3-3 proteins that control the G2/M transition in response to DNA damage, and the WD40 repeat of Cdc4p that regulates S phase entry (Yaffe and Elia, 2001).

In several instances, a phosphopeptide binding domain and a kinase domain are combined within a single molecule, best exemplified by the SH2 domain-containing Src kinases and the Rad53p/Chk2-family of FHA domain-containing kinases. In these proteins, the phosphopeptide binding domain targets the kinase to prephosphorylated (primed) sites, mediates processive phosphorylation at multiple sites within a single substrate, or facilitates kinase activation. Polo-like kinases are distinguished by the presence of a conserved Ser/Thr kinase domain and a noncatalytic C-terminal region composed of two homologous ~70–80 residue segments termed Polo boxes (Sonnhammer et al., 1998). Using a proteomic screen for phosphoserine/threonine binding domains, we recently identified the entire C-terminal region of human Plk1 as a phosphoserine/threonine binding domain, the Polo-box domain (PBD), which appears to target Plk1 to mitotic structures and substrates (Elia et al., 2003).

Humans, mice, and frogs contain three Plk homologs denoted Plk1, Plk2/Snk, and Plk3/Fnk/Prk, while budding yeast, fission yeast, and flies contain only a single Plk family member denoted Cdc5p, Plo1, and Polo, respectively. In addition, humans and mice contain a serine/threonine kinase, Sak, which is an extremely divergent member of the Plk family, containing only a single Polo box and lacking a canonical PBD. The most extensively studied Polo-like kinases, Plk1 and Cdc5p, have been implicated in numerous mitotic processes including activation of Cdc25C and Cdc2-cyclin B at the G2-M transition, centrosome maturation and spindle assembly, cohesin release/cleavage during sister chromatid separation, APC activation during mitotic exit and septin regulation during cytokinesis (Descombes and Nigg, 1998; Nigg, 1998; Glover et al., 1998). In contrast, human Plk2 and Plk3 appear to serve different functions. Plk2 shows peak expression and activity in early G1 (Ma et al., 2003) while Plk3 is activated by several stress response pathways, including DNA damage and spindle disruption (Bahassi et al., 2002; Xie et al., 2001, 2002). In fact, Plk3 plays some roles that may directly antagonize Plk1 function. For example, DNA damage directly inhibits Plk1 (Smits et al., 2000) but activates Plk3 in an ATM-dependent manner (Xie et al., 2001). Consistent with these results, Plk1 overexpression causes oncogenic transformation in NIH 3T3 cells (Smith et al., 1997) while overexpression of Plk3 induces apoptosis (Conn et al., 2000). At present, the mechanisms underlying these functional differences are unknown.

In spite of the variable roles played by different Plk-family members, all require the activity of the Polo-box

*Correspondence: stephen.smerdon@nimr.mrc.ac.uk (S.J.S.), myaffe@mit.edu (M.B.Y.)

[4]These authors contributed equally to this work.

domain for correct subcellular localization (Lee et al., 1998; Ma et al., 2003; May et al., 2002; Reynolds and Ohkura, 2003). Whether the PBDs in other Plks also bind phosphoserine/threonine-containing motifs is not known. Here, we show that the PBDs from human Plk1, 2, and 3, as well as the Plk1 orthologs Plx1 from *Xenopus* and budding yeast Cdc5p all show conserved selection for the core sequence S-[pS/pT]-P/X in oriented peptide library screens. The crystal structure of the human Plk1 PBD in complex with its optimal phosphopeptide motif reveals a mode of binding in which the bulk of the peptide contacts involve a specific lattice of water-mediated hydrogen bonds. Site-directed mutagenesis based on the structural identification of critical phosphothreonine binding residues shows that phosphodependent substrate recognition by the PBD is necessary for Plk targeting to substrates both in vitro and in vivo, and for proper mitotic progression. Furthermore, binding of the optimal Plk1 phosphopeptide to the PBD in full-length Plk1 enhances the in vitro activity of the kinase domain, leading to a model for Plk regulation in which intramolecular inhibition of the kinase by the PBD is relieved by PBD-ligand binding. We conclude that phosphoserine/threonine-dependent binding is a general feature of PBD activity across the Plk family and critically important in Polo-like kinase targeting and regulation.

Results

A Common Consensus Motif Is Recognized by All Plk Polo-Box Domains

Optimal phosphopeptide binding motifs for the PBDs from all members of the human Plk family, *Xenopus* Plx1 and *Saccharomyces cerevisiae* Cdc5p were determined by oriented peptide library screening (Yaffe and Cantley, 2000) (Supplemental Data available at http://www.cell.com/cgi/content/full/115/1/83/DC1). Since we initially isolated the Plk1 PBD in a search for domains that recognize a pThr-Pro-containing motif, primary screens were performed using peptide libraries containing a fixed pThr-Pro core flanked on both sides by four degenerate positions. Each of the five PBD's examined selected for distinct but largely overlapping motifs and all showed unequivocal selection for Ser in the pThr-1 position with selectivity ratios (i.e., the mol% of Ser in the PBD bound peptides at the pThr-1 position divided by the mol% of Ser in the starting library mixture at the pThr-1 position) ranging from 3.0 to 7.5 (Supplemental Tables S1 and S2 available at above website). Motif similarity occurs even though these PBDs vary considerably in amino acid sequence and the respective human Plks perform divergent cellular functions.

Based on these data, secondary peptide libraries containing a fixed Ser-pThr core were used to further refine the motifs and investigate the relative importance of Pro in the pThr+1 position (Supplemental Tables S1 and S2 available at *Cell* website). These data reveal that all Plks investigated, including all conventional human Plk homologs, select a similar motif that can be most generally represented by the consensus sequence:

$$[\text{Pro/Phe}]\text{-}[\phi\text{/Pro}]\text{-}[\phi\text{/Ala}_{\text{Cdc5p}}\text{/Gln}_{\text{Plk2}}]\text{-}$$

$$[\text{Thr/Gln/His/Met}]\text{-Ser-}[\text{pThr/pSer}]\text{-}[\text{Pro/X}]$$

ϕ represents hydrophobic amino acids.

The striking selection observed for Ser in the pThr-1 position in all PBDs was examined in detail for the human Plk1 PBD, which binds to its optimal motif, Pro-Met-Gln-Ser-pThr-Pro-Leu (Supplemental Table S1 available at *Cell* website), with a K_d of 280 nM (Figure 1A). A variety of small side-chain amino acids were therefore substituted in the pThr-1 position, and peptide binding to the Plk1 PBD measured using isothermal titration calorimetry (ITC) (Figure 1A). Surprisingly, conservative replacement of Ser with Gly, Ala, Thr, or Cys, completely abrogated Plk1 PBD-phosphopeptide binding. We had previously observed that replacement of Ser at the pThr-1 position with Val, the amino acid showing the lowest selection in this position, was sufficient to eliminate peptide binding (Elia et al., 2003). Nevertheless, the finding that replacement of Ser with a variety of chemically similar amino acids also completely disrupted the interaction between the PBD and free phosphopeptides in solution was unexpected.

To extend this analysis, each amino acid in the eight positions flanking the pThr within the optimal Plk1 PBD binding motif was substituted with each of the remaining nineteen naturally occurring amino acids using a solid phase array of immobilized phosphopeptides (Figure 1B and Supplemental Data available at *Cell* website). This conclusively demonstrated that only Ser was tolerated in the pThr-1 position. Selectivities at other positions were generally consistent with the results of oriented peptide library screening. Cys and Gly, however, were selected at the pThr+1 position at least as strongly as Pro in the immobilized phosphopeptide assay. These subtle differences most likely reflect the fact that the peptide filter assay examines individual point mutations in the context of a single amino acid sequence, while oriented peptide library screening samples an entire ensemble of sequence motifs simultaneously. Regardless, Pro probably represents the most "physiological" amino acid in the pThr+1 position, since the phosphorylation event necessary for PBD binding is likely to be catalyzed primarily by Pro-directed kinases such as Cdks and MAP kinases.

Overall Structure of the Plk1 PBD

The boundaries of the minimal PBD within the C-terminal regions of both Plk1 and Cdc5p were determined using limited proteolysis. Digestion of the entire C-terminal region of Plk1 (residues 326–603) using V8 protease and trypsin indicated that only the last 45 residues of the linker between the kinase domain and the first Polo box were structured as part of the PBD (Figure 2A and data not shown). Similar results were obtained using the C-terminal segment of Cdc5p (data not shown). We refer to this additional region as the Polo-cap (Pc). For both Plk1 and Cdc5p, we found no significant difference in the phosphopeptide binding affinities of fragments encompassing the entire C-terminal regions or the proteolytically defined PBDs, indicating that the first $\sim$40 amino acids between the kinase and the Pc play no major role in peptide binding. Shorter fragments of both Plk1 and Cdc5p lacking the Pc, were insoluble in *E. coli*, indicating a clear structural role for the Pc in both proteins.

The X-ray structure of a recombinant form of the pro-

A

pT-1 serine analogues abolish Plk1 PBD : peptide binding in solution		
Peptide name	Peptide sequence	K_d
PoloBoxtide-optimal	MAGPMQ-**S**-pT-P-LNGAKK	280 ± 27 nM
PoloBoxtide–7A	MAGPMQ-**A**-pT-P-LNGAYKK	N.D.B.
PoloBoxtide–7G	MAGPMQ-**G**-pT-P-LNGAYKK	N.D.B.
PoloBoxtide–7C	MAGPMQ-**C**-pT-P-LNGAYKK	N.D.B.
PoloBoxtide–7T	MAGPMQ-**T**-pT-P-LNGAYKK	N.D.B.

B

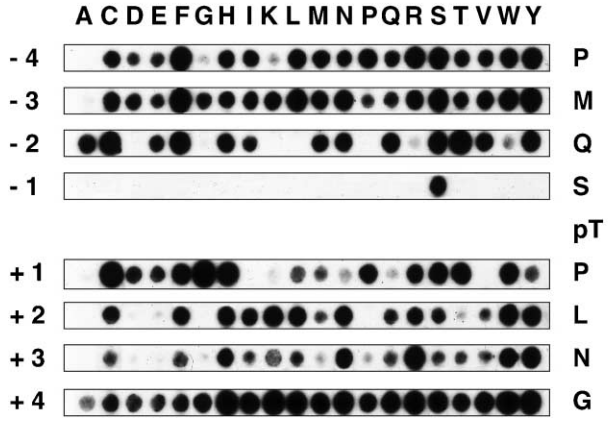

Figure 1. Mutation of the Plk1 PBD Consensus Motif Defines Specificity Requirements for Phosphopeptide Binding

(A) Conservative mutations at the pT-1 serine abolish Plk1 PBD-peptide binding in solution. Isothermal titration calorimetry was used to determine binding affinities. N.D.B. indicates no detectable binding for a Plk1 PBD (residues 326–603) concentration of at least 150 μM. pT denotes phosphothreonine.

(B) Binding of GST-Plk1 PBD (residues 326–603) to a filter array of peptide spots, comprising single point mutants of the Plk1 PBD optimal phosphopeptide (right column). Bound GST-Plk1 was detected by blotting with HRP-conjugated anti-GST antibody.

teolytically defined Plk1 PBD (residues 367–603) in complex with its "optimal" phosphopeptide was solved by multiwavelength anomalous diffraction, and refined at 1.9 Å resolution (Table 1). The structure (Figure 2B) shows that the PBD contains two $\beta_6\alpha$ motifs that comprise the two Polo-box regions (PB1 and 2) identified by sequence profiling. In spite of the fact that the amino acid sequences of the two Polo boxes within any one Plk exhibit only ~20%–25% sequence identity, the structures of the two motifs are quite similar (rms deviation of 77 Cα atoms of 1.6 Å; Figure 2B). The two Polo boxes pack together to form a 12-stranded β sandwich flanked by three α-helical segments (Figure 2C). Although motifs resembling the Polo-box structure are represented in the Protein Databank, the overall domain fold is not. The Pc consists of an α-helical segment αA, loop and short 3_{10} helix that connects to the first β strand of Polo-box 1 (β1) through a short linker region (L1). The Pc wraps around Polo-box 2 tethering it to Polo-box 1. αA packs against αC from PB2 in an antiparallel coiled-coil arrangement, while the 3_{10} helix packs against the shorter αC'. The two Polo boxes are connected by a second ~30 residue linker sequence (L2) that is partially conserved. L1 and L2 run in antiparallel directions between the two Polo-box β sheets. Thus, the hydrophobic core is formed from direct interactions of highly conserved nonpolar residues predominantly located on β1/β2 from PB1 and β6/β7 from PB2, together with an array of interactions with the intercalating linker regions.

Unusual PBD-Phosphopeptide Interactions Are Crucial for Specificity

The phosphopeptide binds in an extended conformation to one end of a shallow cleft formed between the two Polo boxes (Figure 2). In all, ~1000 Å^2 of solvent accessible surface are buried by binding of the seven phosphopeptide residues visible in our electron density maps. Binding involves part of the only highly conserved surface on the PBD (Figures 3A and 3B) explaining the similar motifs selected by different PBDs. The binding site also coincides with the only significant region of positive electrostatic potential (Figure 3C). The phosphopeptide interacts predominantly with β1 from PB1, the N-terminal end of L2 and β8/9 from PB2. Hydrogen-bonding interactions formed with the peptide side- and main-chain atoms alternate to some degree between residues within the two Polo boxes, forming a zipper-like structure at the edge of the PB1/PB2 interface (Figure 3D).

PBD binding to the phosphate moiety involves a combination of direct contacts with protein side-chains and extensive indirect interactions through a well-defined lattice of water molecules, many of which are fully hydrogen-bonded (Figure 3E). In total, the phosphate group

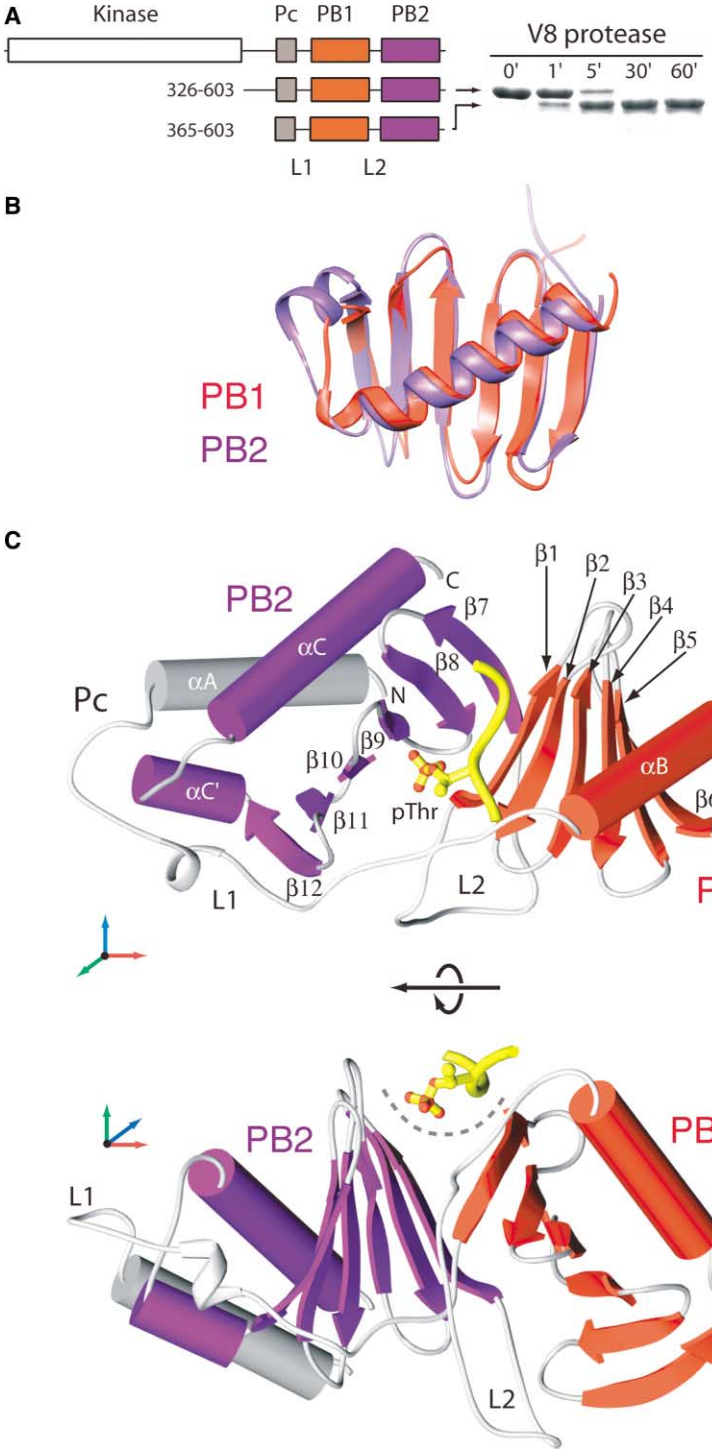

Figure 2. Structure of the Plk1 PBD/Phosphopeptide Complex

(A) Defining the boundaries of the PBD by limited proteolysis. Domain architecture of full-length Plk1 and stable fragments (left) are shown together with the time-course of V8 protease digestion (right). Molecular weight and amino acid boundaries of the limiting domain were determined by mass spectroscopy.

(B) Superposition of the Polo-box 1 and Polo-box 2 $\beta_6\alpha$ structures, colored as in (A).

(C) RIBBONS representation (Carson, 1991) of the structure of the Plk1 PBD in complex with a pThr-containing peptide shown as a ball and stick representation in yellow. The Polo boxes and Polo-cap region are colored as in (A). The phosphopeptide binds at one end of a pocket formed between the two polo boxes.

participates in eight hydrogen-bonding interactions, explaining the critical dependence on phosphorylation for binding (Elia et al., 2003). The only residues that contact the phosphate group directly are His-538 and Lys-540 from PB2, whose side chains form a pincer-like arrangement that chelates the O1, O3, and Oγ phosphate oxygens.

The extraordinarily high selectivity for serine at the pThr-1 position results from a different orientation of the bound phosphopeptide compared with phosphopeptide complexes of 14-3-3 proteins and FHA domains, the two major classes of pSer/pThr binding proteins (Durocher et al., 2000; Yaffe et al., 1997). In these structures, the pThr-1 side-chain is solvent exposed and little selection is observed at this position. In contrast, the peptide orientation in the Plk1 complex is inverted such that the Ser–1 side-chain is directed toward the Plk1

Table 1. Crystallographic Analysis

Dataset (λ Å)	Native (0.98)	Se (0.97838)	Se (0.97887)	Se (0.95)				
Data Collection								
	14.1-SRS		14.2-SRS					
d (Å)	20.0–1.9	20.0–3.5	20.0–3.5	20.0–3.5				
Completeness (%)	97.7	99.9	99.0	99.2				
Redundancy[a]	3.6	3.7[c]	~1.9[c]	~1.9[c]				
R_{sym} (%)[b]	5.3	5.4[c]	5.2[c]	4.9[c]				
Phasing analysis								
Resolution bin (Å)	20–11.2	11.2–7.5	7.5–6.0	6.0–5.2	5.2–4.6	4.6–4.2	4.2–3.9	3.9–3.6
FOM	0.79	0.83	0.79	0.70	0.59	0.53	0.48	0.44
Mean FOM	0.60							
Refinement								
R_{cryst} (%)[d]	R_{free} (%)[e]	rms_{bond} (Å)	rms_{angle} (deg.)					
23.0	25.8	0.007	1.2					

[a] N_{obs}/N_{unique}
[b] $R_{sym} = \Sigma_j|<I> - I_j|/\Sigma<I>$ where I_j is the intensity of the jth reflection and $<I>$ is the average intensity.
[c] Calculated with Bijvoets separated
[d] $R_{cryst} = \Sigma_{hkl}|F_{obs} - F_{calc}|/\Sigma_{hkl} F_{obs}$
[e] R_{free} – as for R_{cryst} but calculated on 5% of the data excluded from the refinement calculation.

surface (Figure 3B). In this orientation, it engages in two hydrogen bonding interactions with Trp-414 main-chain atoms, and one with the Leu-491 main-chain carbonyl via a water molecule (Figure 3D). Significantly, the Ser–1 Cβ atom makes favorable van der Waals interactions with Cδ1 from the Trp-414 indole side-chain. This explains why even a conservative replacement with Thr abrogates peptide binding (Figure 1A), presumably due to a steric clash of the additional γ-methyl group with Trp-414. In addition, the absolute conservation of Trp-414 predicts that all family members should exhibit the same serine preference, and this is, indeed, the case.

The critical role of Trp-414 in ligand binding revealed by our crystal structure (Figure 3D) explains the observation that a W414F mutation eliminates both centrosomal localization of Plk1 and its ability to complement the *cdc5-1 ts* (Lee and Erickson, 1997). Both of these effects are likely to be at least partly attributable to disruption of critical Ser-1 interactions with the PBD. In agreement with this, a mutant PBD containing the W414F substitution is severely compromised in phosphopeptide binding, with an affinity of >100 μM as determined by ITC. Loss of binding does not result from gross structural perturbation of the Polo-box fold, since the mutant and wild-type PBDs show similar CD spectra (data not shown).

Consistent with the library selection, the protein-peptide interface is dominated by interactions of the PBD with the pThr and Ser-1 (Figures 3C and 3D). Although we observed modest selection for Pro at the pThr+1 position, the structure shows limited contribution to the binding interface, and multiple substitutions at this position are tolerated for peptide binding (Supplemental Tables S1 and S2 available at *Cell* website; Figure 1B). In the PBD structure, the *trans*-proline introduces a kink after the Ser-pThr directing the peptide backbone back toward the binding surface, allowing the pThr+2 main chain amino group to contact the PBD. Thus, the +1 Pro likely increases binding affinity by diminishing the entropic penalty for making this favorable backbone contact. This contrasts with structures of pSer-Pro and pThr-Pro peptide complexes with the Pin1 WW and the Cdc4 WD40 domains, respectively, in which the Pro+1 side chain inserts into a hydrophobic pocket and makes coplanar interactions with a buried tryptophan (Orlicky et al., 2003; Verdecia et al., 2000).

Plk1 and Sak Polo Boxes Are Structurally Distinct—One Motif, Two Folds

The human Plk family encompasses the canonical kinases (Plks 1–3) and Sak, which contains a highly homologous Ser/Thr kinase domain but only a single divergent Polo box. Recent structural data has shown that the isolated Polo box from murine Sak forms an intermolecular dimer, leading to the suggestion that tandem Polo boxes in Plk1-related Plks may form a related, intramolecular "dimeric" architecture (Leung et al., 2002). Our structure shows that this notion is broadly correct. In each case, the Polo-box repeat comprises a six-stranded β sheet and α-helix, that associates with a second Polo-repeat via intra- or intermolecular interactions in Plk1 and Sak respectively, to form β sandwich domain structures. However, closer examination reveals profound differences between the organization of the two structures (Figure 4). Most strikingly, the association of the two Polo boxes differs completely such that residues forming the interface between Polo repeats in the Sak homodimer are located largely on the exterior of the Plk1 β sandwich, where they partially form the interface with the flanking α-helical segments. The grossly different architectures argue against conservation of phosphoprotein binding function since residues most intimately involved in phosphopeptide binding by Plk1 (e.g., His-538/Lys-540, Trp-414) are not conserved in Sak. Furthermore, the electrostatic potential surface of the Sak Polo-box dimer shows no significant regions of positive charge (data not shown), a property otherwise common to phosphodependent binding proteins. Ex-

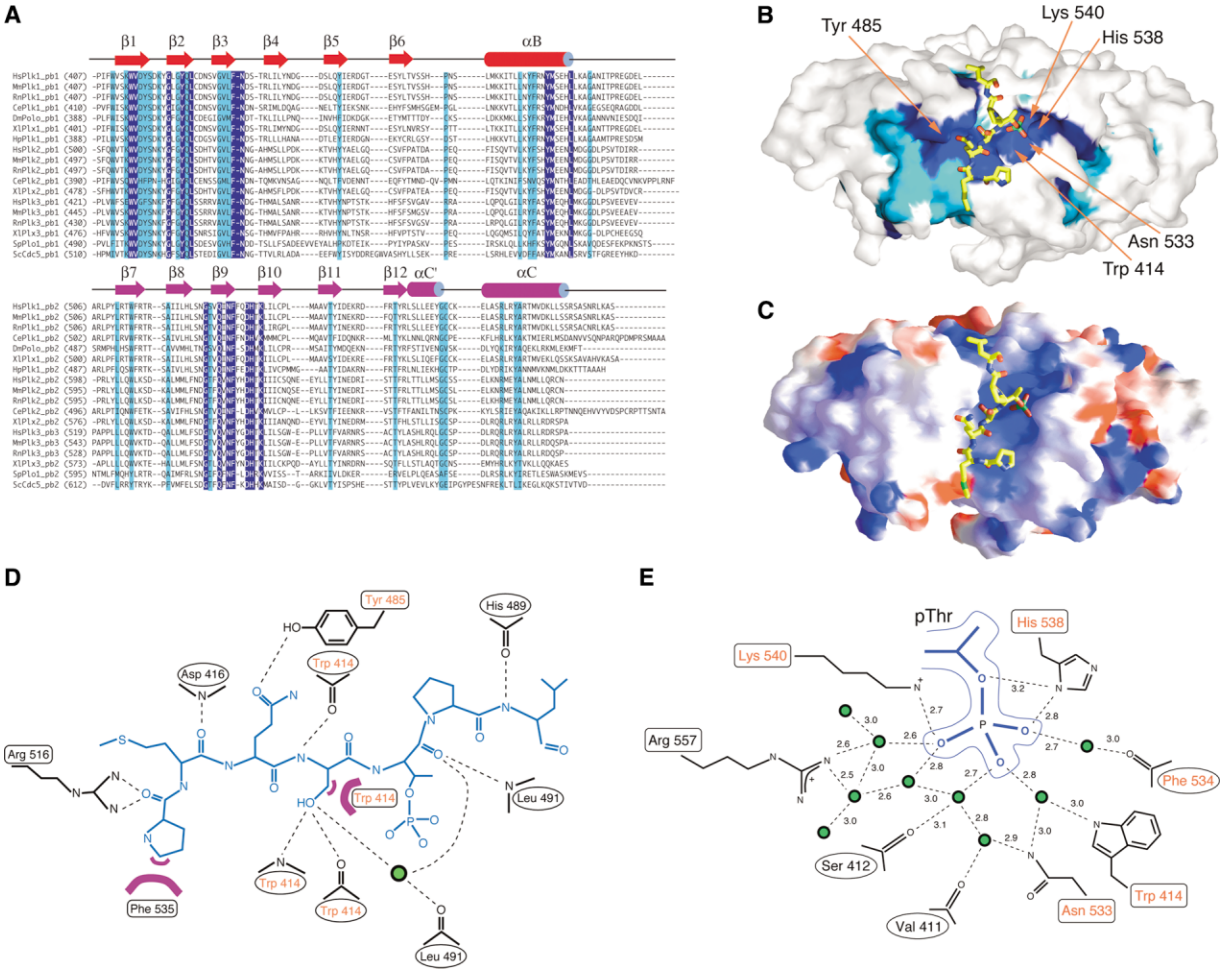

Figure 3. Details of the Plk1 PBD/Phosphopeptide Interaction

(A) Structure-based sequence alignment of the Polo-box domain family. Residues with 100% conservation are shaded purple while highly conserved residues are shaded cyan.

(B) The most highly conserved residues within the Plk1 PBD are located exclusively on the peptide binding face of the PBD. The coloring scheme is as in (A).

(C) Electrostatic potential of the PBD phosphopeptide pocket, calculated using GRASP (Nicholls et al., 1991), with the phosphopeptide superimposed in stick representation (oxygen atoms, red; nitrogen atoms, blue). Negative potential of the PBD surface is colored red and positive potential blue.

(D) Schematic representation of the interactions between the phosphopeptide (blue) and the Plk1 PBD. Hydrogen bonds, van der Waals interactions, and water molecules are denoted by dotted lines, purple crescents, and green circles, respectively.

(E) Schematic representation of direct and indirect hydrogen bonds (dotted lines) between the phosphate and the Plk1 PBD. Hydrogen bond lengths are given in angstroms.

periments to determine whether the Sak Polo-box dimer is able to bind to phosphopeptides are underway.

Mutation of the His-Lys Pincer Abolishes Phosphopeptide Binding In Vitro, Cdc25 Binding In Vivo, and Centrosomal Localization of the Plk1 PBD

To verify that the key pThr-interacting residues identified in the X-ray crystal structure are responsible for mediating phosphodependent interactions in vitro and in vivo, we mutated His-538 and Lys-540 of the pThr pincer motif (Figure 5A). Mutation of His-538 to Ala reduced binding of in vitro translated Plk1 PBD to a bead-immobilized pThr-Pro oriented library by ~50%. Mutation of Lys-540 to Met, as a conservative structural replacement for a partially buried lysine, reduced binding by ~95%, though a small amount of phosphospecific binding was still observed. Mutation of both His-538 and Lys-540 eliminated phosphopeptide binding completely as shown using both a bead-immobilized pThr-Pro oriented library (Figure 5A) and by ITC (Figure 5B).

During mitotic entry, Cdc2/Cyclin B and Plk1 cooperate to activate the dual specificity phosphatase Cdc25 through extensive phosphorylation of its N terminus as part of an amplification loop for Cdc2/Cyclin B activation (Abrieu et al., 1998; Kumagai and Dunphy, 1992). Mitotically phosphorylated Cdc25C exhibits a large mobility shift on SDS-PAGE (Kumagai and Dunphy, 1992) (brackets labeled "P" in Figures 5C–5E), while Cdc25C in noncycling cells or cells arrested in G1/S with aphidicolin exhibit two lower mobility forms (brackets labeled "U" in Figures 5C–5E). Cdc25C is phosphorylated on at least

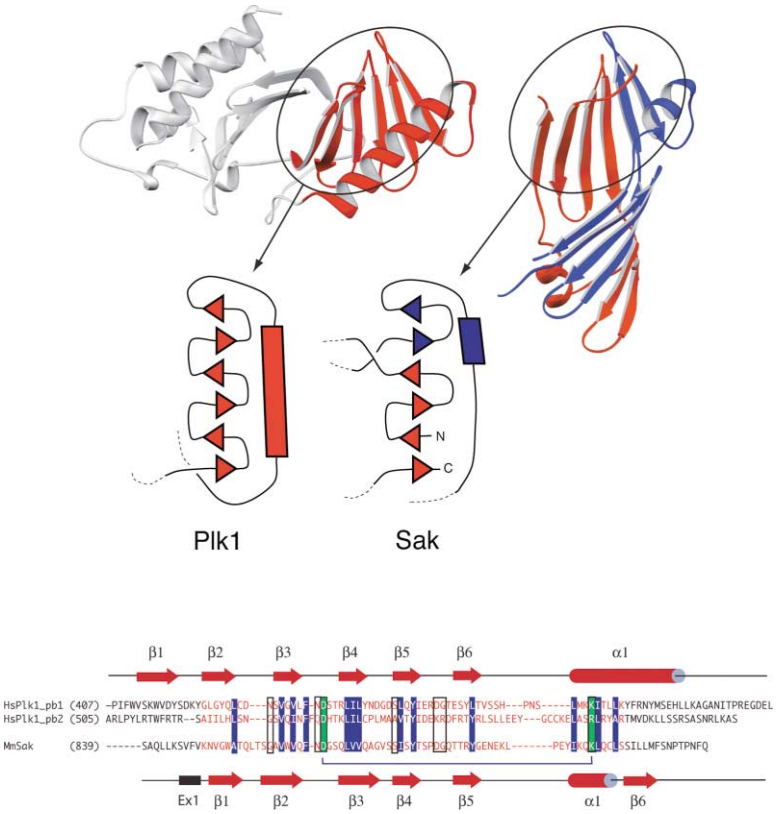

Figure 4. Topologies of the Polo Boxes from Plk1 and Sak

(A) Comparison of the β sandwich folds of the Plk1 PBD and the Sak Polo-box dimer. Tertiary structures are shown on the top together with secondary structure topology (triangles, β strands; rectangles, α helices) on the bottom. PB1 of Plk1 is colored red while the two Polo boxes of the Sak homodimer are shown in red and blue, respectively. The $\beta_6\alpha$ topology of the Plk1 Polo box is replaced by a circularly permuted $\beta_5\alpha\beta$ topology in Sak. Consequently, Plk1 β1 has no equivalent in the Sak Polo-box sequence and instead overlaps structurally with Sak β6. In addition, the Sak β sheet is completed by a "segment-swap" of β4 and 5 between monomers.

(B) Sequence alignment of the Polo boxes from Plk1 and Sak. β sheet and α-helix notation follows PB1; the corresponding elements for PB2 are β7 through β12 and αC. A conserved salt-bridging interaction, initially observed in the Sak structural analysis (Leung et al., 2002), is shown by the bracket with the basic and acidic residues highlighted in green. Conserved nonpolar residues are highlighted in blue and residues conserved between Sak and at least one of the Plk1 PBDs are boxed.

five Ser/Thr-Pro sites by Cdc2/Cyclin-B in vitro (Izumi and Maller, 1993; Strausfeld et al., 1994). One of these sites, Thr-130, occurs within a near-optimal PBD binding motif, Leu-Leu-Cys-Ser-pThr-Pro-Asn. We previously observed that a GST-fusion of the isolated PBD could pull down wild-type Cdc25C, but not a T130A or S129V Cdc25C mutant, from mitotically arrested HeLa cell lysates. These data strongly suggested that Cdk priming of Thr-130 generates a binding site for the Plk1 PBD to facilitate subsequent activation of Cdc25C by Plk1-mediated phosphorylation (Elia et al., 2003). As shown in Figure 5C, expression of His-Xpress-tagged wild-type Plk1 PBD in vivo results in a strong interaction primarily with the mitotically phosphorylated form of endogenous Cdc25C in nocodazole-arrested HeLa cells. However, expression of the His-538/Lys-540 pincer mutants eliminates Cdc25C binding as also observed in cells transfected with a PBD construct lacking the second Polo box (residues 326–506).

To investigate whether the PBD plays a similar substrate-targeting role in full-length Plk1, HeLa cells were transfected with myc-tagged wild-type or mutant full-length Plk1, and interactions between Plk1 and endogenous Cdc25C examined in nocodazole-arrested cells by immunoprecipitation (Figure 5D and Supplemental Data available at *Cell* website). We observed a strong in vivo interaction between the mitotically upshifted form of endogenous Cdc25C with full-length Plk1 in arrested cells that, surprisingly, was not increased when a kinase-dead Plk1 mutant (K82R) or a double mutant incorporating a T210D mutation in the T-loop to further expose the substrate binding cleft were employed as substrate traps. Conversely, mutation of the His-538/Lys-540 pincer in full-length Plk1 completely disrupted the in vivo interaction between Plk1 and Cdc25C demonstrating that the interaction of the full-length molecules in G2/M-arrested cells is mediated primarily through the PBD. This result is important since it directly demonstrates a requirement for PBD phosphopeptide binding in substrate targeting in the context of the full-length Plk1 molecule. We did observe a small amount of binding of the nonmitotically phosphorylated form of Cdc25C to both the isolated PBD and full-length Plk1 (Figures 5C and 5D), consistent with the fact that Cdc25C can serve as a Plk1 substrate even in the absence of Cdk phosphorylation (Kumagai and Dunphy, 1992), albeit presumably less efficiently.

Finally, we observed that mutation of the His-538/Lys-540 pincer eliminates targeting of the Plk1 PBD to centrosomes in permeabilized prophase-arrested cells (Figure 5F). This finding suggests that the localization of Plk1 to centrosomes observed in vivo (Jang et al., 2002; Lee et al., 1998) results from direct interactions between the PBD and phosphorylated centrosomal components. In summary, these data show conclusively that the structurally defined His-538/Lys-540 pincer mechanism that is responsible for mediating phosphopeptide binding in vitro, plays a similarly critical role in substrate targeting in vivo.

Phosphodependent Substrate Recognition Is Necessary for the Disruption of Mitotic Progression by the Isolated Plk1 PBD

Since the PBD is necessary for targeting Plk1 to primed substrates, its overexpression might be expected to act in a dominant-negative fashion to inhibit correct local-

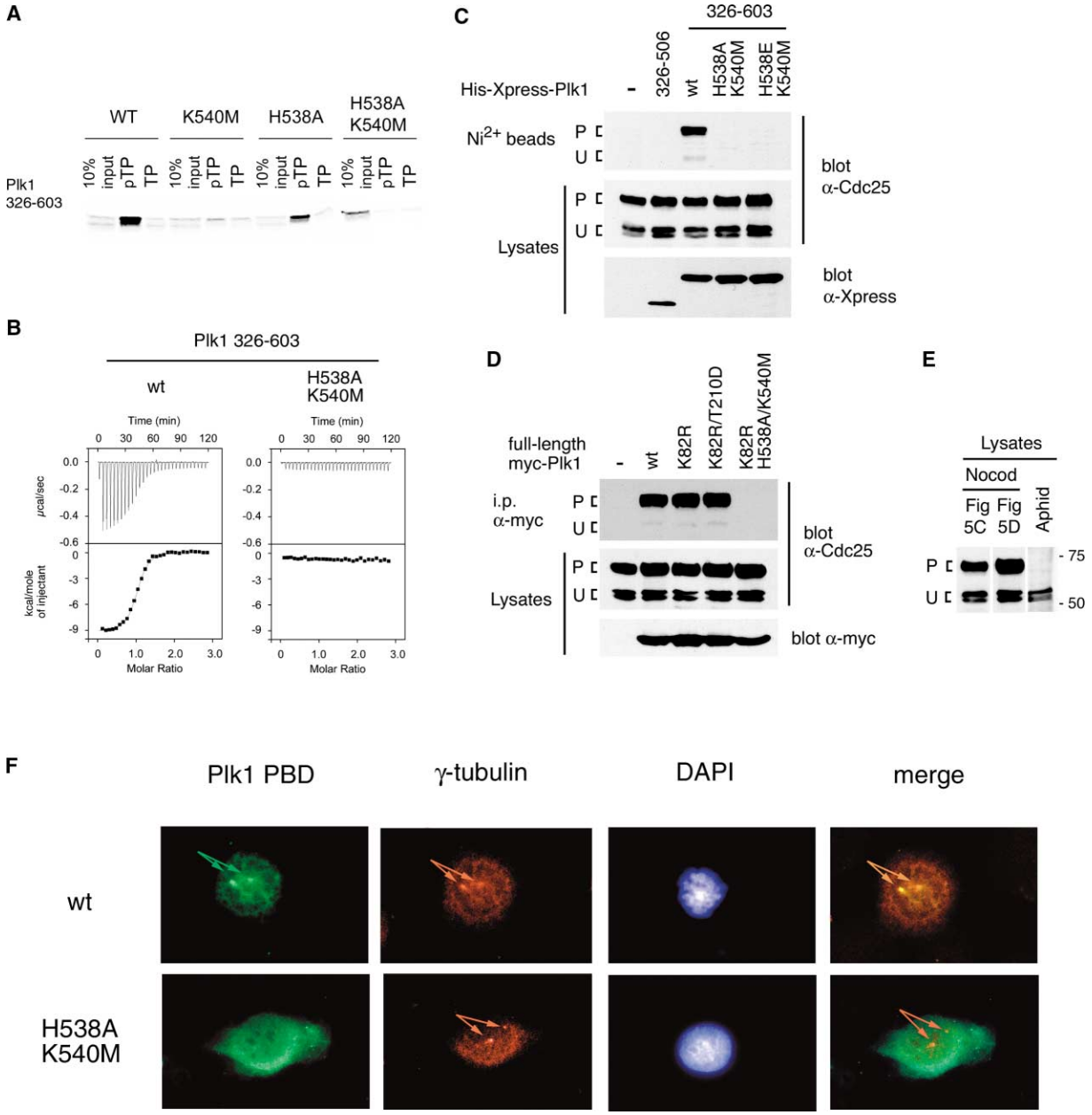

Figure 5. Mutation of the H538/K540 Pincer Sequence within the Plk1 PBD Abolishes Phosphopeptide Binding In Vitro and Cdc25 Binding In Vivo

(A) Wild-type and mutant Plk1 PBD (residues 326–603) were translated in vitro in the presence of ^{35}S-methionine and examined for binding to an immobilized pThr-Pro-oriented library (pTP) and its unphosphorylated counterpart (TP).

(B) H538A/K540M mutation of the Plk1 PBD abolishes binding to its optimal phosphopeptide as measured by isothermal titration calorimetry.

(C) Mutation of the H538/K540 pincer disrupts interaction of the isolated Plk1 PBD with Cdc25 in vivo. HeLa cells were transfected with wild-type and mutant versions of a His-Xpress-tagged Plk1 PBD construct (residues 326–603) or with a control Plk1PBD construct lacking the second Polo box (residues 326–506). Cells were arrested in G2/M with nocodazole, the Plk PBD pulled down with NTA beads, and bound endogenous proteins analyzed by SDS-PAGE. Immunoblots revealed preferential association of the PBD with the mitotically hyperphosphorylated form (P) of Cdc25C compared with hypophosphorylated form (U).

(D) Mutation of the H538/K540 pincer in the Plk1 PBD disrupts interaction of full-length Plk1 with Cdc25 in vivo. HeLa cells were transfected with wild-type and mutant versions of full-length myc-tagged Plk1 and arrested in G2/M with nocodazole. Plk-myc was immunoprecipitated with anti-myc-conjugated beads and Cdc25 binding to Plk1 analyzed as in (C).

(E) Hyper- and hypophosphorylated forms of Cdc25C. Lysates used in (C) and (D), along with a control lysate arrested in G1/S with aphidocolin, were immunoblotted for Cdc25C.

(F) Centrosomal localization of the Plk1 PBD in HeLa Cells-U2OS cells were arrested in G2/M with nocodazole and then incubated with wild-type or mutant GST-Plk1 PBD. Overlap of the GST and γ-tubulin signals is shown in the merged panel.

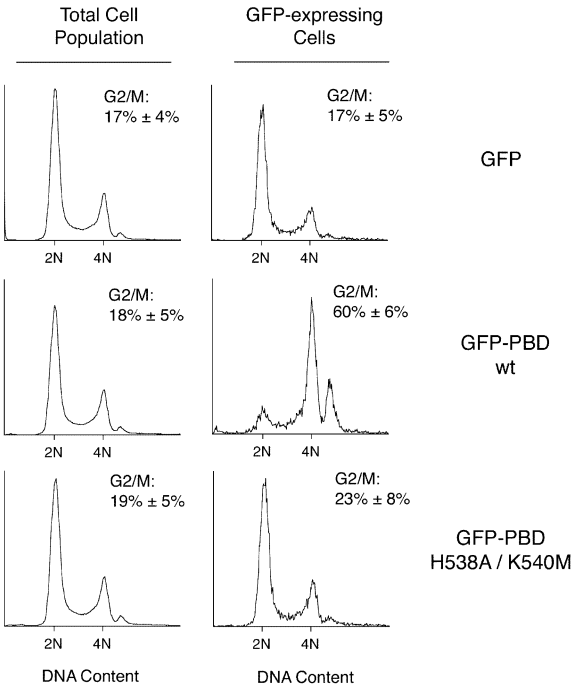

Figure 6. Mutation of the H538/K540 Pincer Prevents G2/M Arrest and Aneuploidy Resulting from Overexpression of the Plk1 PBD in HeLa Cells

HeLa cells were transfected with wild-type and mutant GFP-tagged Plk1. Cells were harvested, stained with Hoechst 33342, and analyzed by FACS to determine DNA content in the total cell populations (left images). Similar analysis of the transfected cell population only was performed by gating only on the GFP expressing cells (right images). Percentages are averages from three independent experiments.

ization of endogenous Plk1 and, thus, disrupt Plk1 function. Indeed, overexpression of the C terminus of Plk1 has been shown to cause mitotic arrest and induce formation of randomly oriented, disorganized spindles (Jang et al., 2002; Seong et al., 2002). In agreement with previous studies, we found that overexpression of a GFP-fusion of the Plk1 PBD in HeLa cells caused a dramatic increase in the population of cells in G2/M (60% for PBD-GFP versus 17% for GFP-expressing cells) (Figure 6). Importantly, this accumulation of mitotic cells was abolished by mutation of His-538 and Lys-540 (23% in G2/M). In addition, expression of the wild-type PBD-GFP construct induced aneuploidy in HeLa cells, evident as a peak of cells with DNA content >4N, in agreement with anti-Plk1 antibody microinjection studies (Lane and Nigg, 1996). However, this effect was completely lost when the His/Lys pincer mutant was employed. The dominant-negative effects strongly suggest that phosphopeptide binding by the PBD in full-length Plk1 normally plays a role in both proper mitotic progression and in the establishment of a functional bipolar spindle to ensure equal chromosome segregation.

Phosphopeptide Binding to the PBD Stimulates Plk1 Kinase Activity

Deletion of the C terminus of Plk1 has been observed to increase the kinase activity ~3-fold (Lee and Erikson, 1997; Mundt et al., 1997) while the isolated Plk1 C terminus interacts with and inhibits the activity of the isolated kinase domain in *trans* (Jang et al., 2002). Here, we show that the kinase domain appears to inhibit phosphopeptide binding by the PBD. While the isolated Plk1 PBD binds strongly and specifically to pSer/pThr-containing peptides (Figure 5A), phosphopeptide binding by the PBD within full-length Plk1 is reduced at least 10-fold and is considerably less phosphodependent (Figure 7A, wt lanes). However, the limited phosphospecific binding component of full-length Plk1 is clearly mediated by the PBD (Figure 7A, compare wt pTP and TP lanes with H538A/K540M pTP and TP lanes). This suggests that a mutually inhibitory interaction exists between the Plk1 PBD and the kinase domain in full-length Plk1. We wondered whether binding of the PBD to phosphopeptides was sufficient to relieve this intramolecular interaction and stimulate kinase activity. As shown in Figure 7B, addition of the optimal PBD phosphopeptide increased recombinant Plk1 kinase activity by a factor of 2.6, while addition of the nonphosphorylated peptide had no effect. This result is comparable to the ~2.5-fold stimulation of full-length Src-family kinase activity that is observed when incubated with their optimal SH2 binding phosphotyrosine peptides (Liu et al., 1993; Moarefi et al., 1997). Thus, our results for Plk1 suggest that binding of the PBD to primed phosphorylation sites not only serves to target the kinase domain to substrates but also simultaneously activates the kinase domain for substrate phosphorylation by relieving an inhibitory intramolecular interaction (Figure 7D). The interaction between the kinase domain and the PBD does not appear to involve the phosphopeptide binding site, since the isolated kinase domain binds to both wild-type and H538A/K540M mutant PBDs in *trans* (Figure 7C).

Discussion

Structural Definition of the Polo-Box Domain: A Specialized Phosphoprotein Recognition Module

Previous reports have described the presence of 1–3 Polo boxes within the C-terminal regions of Polo-like kinases (Glover et al., 1998; Nigg, 1998; Seong et al., 2002). Our X-ray structure now shows that the PBD consists of two structurally homologous regions corresponding to two conserved Polo-box sequences. Phosphopeptide binding occurs at the interface of the two Polo boxes, rationalizing both the observed 1:1 stoichiometry of PBD/ligand binding (Figure 5B) and the requirement for both Polo boxes for Plk1 localization in vivo (Seong et al., 2002). Polo-box domains now join an expanding family of pSer/pThr binding domains that includes 14-3-3 proteins, WW, FHA, WD40, and Smad MH2 domains (Yaffe and Smerdon, 2001). In contrast to other more ubiquitous phosphodependent binding modules, PBDs occur only in Polo-like kinases where they localize Plks to specific subcellular organelles and mitotic structures (Jang et al., 2002; Lee et al., 1998, 1999).

Common Phosphopeptide Motif Selection by the PBD Family

In higher eukaryotes, different Plk family members function at different points in the cell cycle or play antagonis-

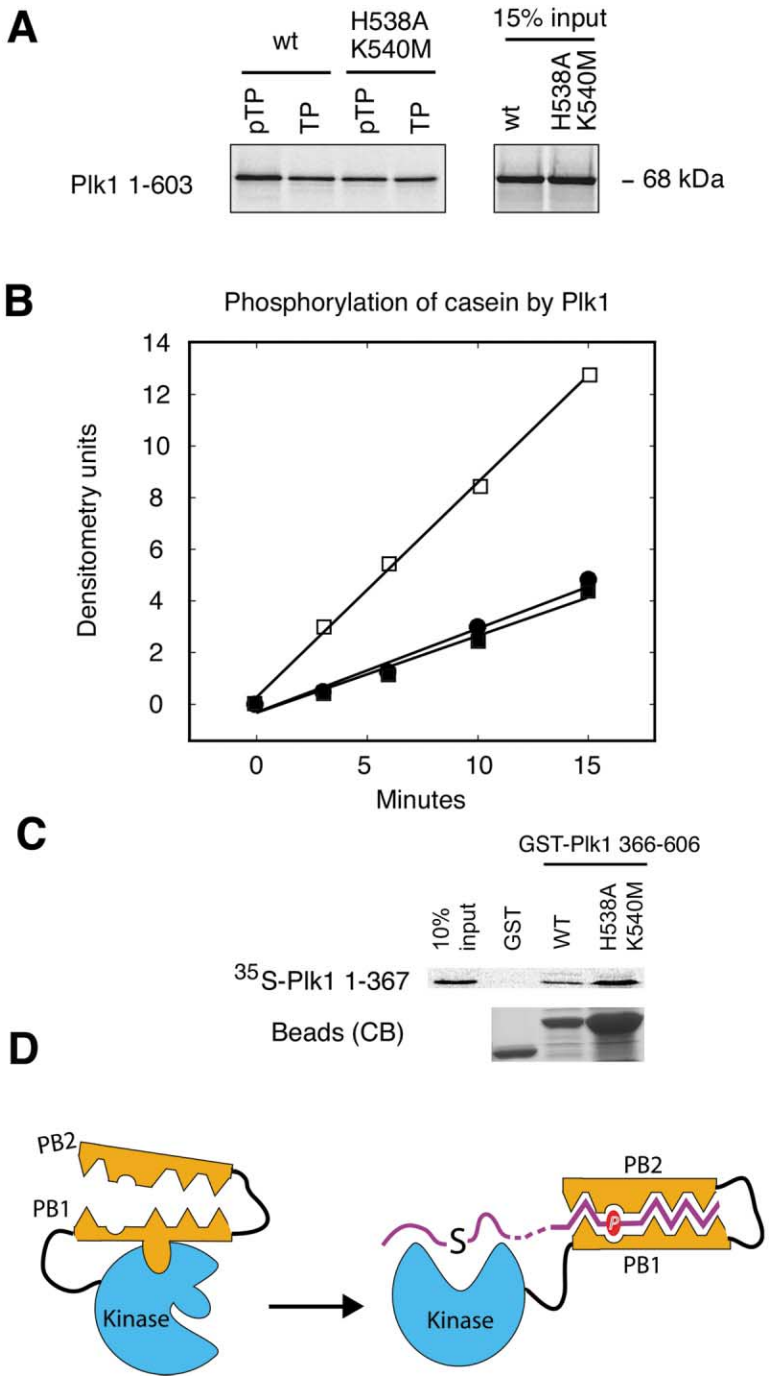

Figure 7. Intramolecular Inhibition of the Plk1 Kinase Domain by the PBD Is Relieved by Ligand Binding.

(A) Phosphopeptide binding by full-length Plk1 is reduced relative to that for the isolated Plk1 PBD. Approximately 10% of input full-length Plk1 (residues 1–603) interacted with an immobilized pThr-Pro oriented library with slight preference over the unphosphorylated library analog in multiple experiments. The phosphodependent binding component arose from the PBD, as it was eliminated by mutation of the His538/K540M pincer. In contrast, phosphopeptide binding by the isolated PBD (Figure 5A) was 10-fold greater and considerably more phosphodependent.

(B) The optimal PBD phosphopeptide stimulates full-length Plk1 kinase activity. GST-Plk1 (prepared in SF9 cells) was preincubated without peptide (closed circles), with 250 μM of the optimal PBD phosphopeptide (open squares) or with 250 μM of the nonphosphorylated optimal peptide counterpart (closed squares) for 5 min at room temperature prior to initiating the kinase reaction by addition of ATP. [^{32}P]-incorporation into casein was determined by SDS-PAGE electrophoresis, autoradiography, and densitometry.

(C) The Plk1 kinase domain binds the PBD at a site distinct from the phosphopeptide binding pocket. The kinase domain was translated in vitro in the presence of ^{35}S-methionine and incubated with beads containing wild-type or mutant GST-PBD, or GST alone (bottom image). Bound proteins were analyzed by SDS-PAGE/autoradiography (upper image).

(D) A model for Plk1 regulation by the PBD. PB1 and PB2 are shaded orange, kinase domain cyan, phosphopeptide purple with phosphate in red. Inhibitory interactions between the PBD and the kinase domain in the basal state (left) are relieved by phosphopeptide binding (right).

tic roles in response to DNA damage. Given the similarity in the selected motifs for these three proteins, how do individual Plks achieve substrate specificity? Potential mechanisms include different substrate selectivities by their kinase domains, spatially and/or temporally restricted activation of Plks by upstream kinases, or the well documented cell-cycle regulation of Plk1 and 2 expression (Golsteyn et al., 1994; Lee et al., 1995; Ma et al., 2003).

In addition to pThr-1 selectivity for serine, all PBDs that we have examined exhibit some specificity for proline at the pThr+1 position, emphasizing a central role for Cdks and other proline-directed kinases in priming substrates for Plk1 targeting. Several lines of evidence support this model. For example, maximal Plk1-induced activation and nuclear translocation of Cdc25 has been shown to require cyclin B coexpression (Toyoshima-Morimoto et al., 2002). Furthermore, full reconstitution of purified APC activity requires prior synergistic phosphorylation of the APC by both Cdc2 and Plk1 (Golan et al., 2002). Nevertheless, a tolerance for residues other than proline demonstrates that other mitotic kinases may also serve as priming agents. In this regard, the NIMA-related kinase Fin1 has been recently shown to

increase Plo1 affinity for spindle pole bodies in *S. pombe* (Grallert and Hagan, 2002). Identification of substrates for Plk family members, as well as the kinases involved in substrate priming will be crucial in clarifying many of these issues.

A Model for Phospholigand-Induced Plk Activation

Two alternative models for intramolecular regulation of kinase activity by a phosphopeptide binding domain are exemplified by Src-family kinases and SHP-family tyrosine phosphatases. In the Src model, the phosphopeptide binding cleft of the SH2 domain engages an internal phosphotyrosine motif at the C terminus of the molecule to hold the kinase domain in an inactive conformation (Sicheri et al., 1997; Xu et al., 1997). Plk1 does not appear to operate through this mechanism since it does not possess an internal optimal PBD binding site. Moreover, interaction of the PBD with the Plk1 kinase domain is not dependent on kinase domain phosphorylation (Jang et al., 2002) and mutation of Thr-210 to Asp as a mimic of activation loop phosphorylation, actually abolishes PBD binding (Jang et al., 2002). Since the His-Lys pincer mutations that disrupt phosphodependent interactions do not affect PBD-kinase interactions (Figure 7C), it would seem that inhibition occurs through phosphoindependent binding by the PBD.

In the SHP2 model, binding of the N-terminal SH2 domain to the phosphatase domain partially occludes the catalytic cleft and deforms the SH2 domain's binding pocket, reducing its phospholigand affinity (Hof et al., 1998). This effect resembles the reduced phosphopeptide binding that we observe for the PBD in the context of full-length Plk1 (Figure 7A). In the case of SHP2, high local concentrations of phosphotyrosine ligands are able to bind to the N-terminal SH2 domain, inducing a conformational rearrangement of the binding cleft. This is transmitted to its phosphatase-interacting surface and releases the catalytically competent phosphatase domain. We believe Plks may be regulated by a related mechanism (Figure 7D). Examination of the crystallographic temperature factors of the Plk1 PBD implies a dynamic association of the two Polo boxes that is, presumably, more pronounced in the absence of the phosphopeptide ligand. Phosphopeptide binding may therefore act as a structural switch, stabilizing a PBD conformation that is inappropriate for association with the kinase domain. Subsequent Thr-210 phosphorylation by upstream kinases would then maintain the active state by preventing rebinding of the PBD to the kinase. Proof or otherwise of this mechanism will require further structural and biochemical analyses of full-length Plks and their complexes.

The Structural Basis of Phosphopeptide Binding

The PBD binds to phosphorylated epitopes in a way that is distinct from that observed previously in structures of other protein-phosphopeptide complexes (Yaffe and Smerdon, 2001). Although stereospecific, solvent-mediated binding has been described in other systems, such extensive "solvent-bridged" interactions with the phosphoryl group are not observed in other protein-phosphopeptide complexes where the phospho moiety is held by direct interactions, usually with conserved arginine side-chains. The importance of the Plk1 His/Lys pincer is exemplified by our observations that mutation abrogates phosphopeptide binding in vitro, targeting of Plk1 to Cdc25C in vivo, and centrosomal localization, as well as disrupting the ability of the isolated PBD to induce G2/M arrest and aberrant spindle function. Recently, downregulation of human Plk1 has been shown to inhibit proliferation of cultured tumor cells (Elez et al., 2000; Liu and Erikson, 2003), indicating that Plks are potentially important targets for therapeutic intervention. The unique pattern of interactions with the Ser-pThr dipeptide suggest that this motif may now be employed as a template for the design of antiproliferative inhibitors specifically directed against Polo-box domains.

Experimental Procedures

Cloning and Expression of PBD Proteins

C-terminal fragments of human Plk1 (residues 326–603), human Plk2 (residues 355–685), human Plk3 (residues 335–646), *Xenopus* Plx1 (residues 317–598), and *Saccharomyces cerevisiae* Cdc5p (residues 357–705) were amplified from IMAGE cDNA clones or *S. cerevisiae* chromosomal DNA by PCR and ligated into suitably digested pGEX4T-3 or pGEX-6P1 (Pharmacia). Point mutations were introduced using the QuikChange mutagenesis kit (Stratagene). Proteins were expressed in *E. coli* BL21(DE3) cells and purified by glutathione-affinity chromatography. For measurements of peptide binding affinity and domain-mapping experiments, proteins were cleaved from GST with either thrombin or viral protease 3C (Pharmacia-LKB) and further purified by anion exchange chromatography or gel filtration.

Domain Mapping and Protein Purification

Limited proteolysis of Plk1 (residues 326–603) and Cdc5p were performed using trypsin or endoproteinase Glu-C (Promega). N- and C-terminal limits were determined by Edman sequencing and electrospray mass spectrometry. DNA sequences encoding the proteolytically defined domains were amplified by PCR and cloned into pGEX-6P1 (Cdc5p) or a version modified to allow ligation-independent cloning (S.J.S., unpublished data). Recombinant PBDs were then expressed and purified as above.

Crystallization and Structure Determination

For crystallization, the phosphopeptide MAGPMQSpTPLNGAYKK was mixed with the Plk1 PBD fragment in a 1.5:1 stoichiometric excess and concentrated to ~0.2 mM in a buffer containing 20 mM Tris·HCl [pH 8.0]/500 mM NaCl, 1 mM EDTA, and 3 mM DTT. Crystals were grown by microbatch methods at 18°C and belong to monoclinic space-group $P2_1$ ($a = 62.4$ Å, $b = 79.5$ Å, $c = 62.0$ Å, $\beta = 93.3°$) with two complexes per asymmetric unit. Native data were collected on Station 14.1 at the SRS, Daresbury (United Kingdom) using cryopreserved crystals at a temperature of 100°K. All data were reduced using the HKL suite of processing software (Otwinowski and Minor, 1997). Phase information was derived from a three wavelength MAD experiment, using a single, plate-like crystal of Se-methionine substituted PBD in complex with the phosphopeptide. Data for each wavelength were collected to 3.5 Å spacing on Station 14.2 at the SRS, Daresbury. Ten Se sites (five per monomer) were located, and the phases refined using SOLVE (Terwilliger and Berendzen, 1999). Phases were extended to ~2.5 Å against the native data using real-space noncrystallographic symmetry averaging in RESOLVE (Terwilliger and Berendzen, 1999). These maps allowed a nearly complete model of the PBD, together with seven residues of the phosphopeptide to be built using "O" (Jones et al., 1991). Subsequent refinement using native data to 1.9 Å was carried out using Refmac 5.0-ARP/wARP from the CCP4 suite. A summary of crystallographic statistics is shown in Table 1.

Centrosomal Localization of the Plk1 PBD

U2OS cells were cultured in 8-well chamber slides and cycling cells arrested in G2/M by treatment with nocodazole (50 ng/mL) for 14

hr. After rinsing with PBS, cells were incubated with 4 μM GST-Plk1 PBD (residues 326–603) and Streptolysin-O (1 U/ml) in permeabilization buffer (25 mM HEPES [pH 7.9], 100 mM KCl, 3 mM NaCl, 200 mM sucrose, 20 mM NaF, and 1 mM $NaOVO_4$) for 20 min at 37°C. Cells were fixed in 3% paraformaldehyde/2% sucrose for 10 min at RT and extracted with a 0.5% Triton X-100 solution containing 20 mM Tris·HCl [pH 7.4], 50 mM NaCl, 300 mM sucrose, and 3 mM $MgCl_2$ for 10 min at RT. Slides were stained with Alexa Fluor 488-conjugated anti-GST (Molecular Probes) and monoclonal anti-γ-tubulin (Sigma) antibodies at 4°C overnight, then stained with a Texas Red-conjugated antimouse secondary antibody for 60 min at RT and counterstained with 4 μg/ml DAPI. Images were analyzed using NIH Image.

Cell-Cycle Analysis

HeLa cells were transfected with wild-type and mutant forms of GFP-tagged Plk1 (residues 326–603) for 32 hr. Media containing floating cells was retained, and attached cells were released from plates by trypsinization. The two cell populations were combined, washed with PBS, and stained with Hoechst 33342 (10 μg/mL) for 30 min at 37°C in DMEM/10%FBS (1×10^6 cells/mL). Dead cells were stained by incubation with propridium iodide (5 μg/mL) for 5 min at 4°C. Fluorescent signals were quantitated on a FAC Star Plus (Becton Dickinson) cell-sorting machine using Cell Quest software. Cell cycle analysis of total live cells (no propidium iodide staining) and live GFP-expressing cells (no propidium staining and GFP positive) was performed using Modfit 2.0.

Acknowledgments

We are grateful to A. Amon for Cdc5; R. Erikson for baculovirus constructs of GST-Plk1; S. Gamblin for assistance with crystal handling and data collection; D. Lowery for assistance with cloning; and S. Gamblin, K. Rittinger, and I. Manke for critical reading of the manuscript. This work was supported, in part, by NIH grant GM60594 and a Burroughs-Wellcome Career Development Award to M.B.Y.

Received: June 4, 2003
Revised: September 2, 2003
Accepted: September 2, 2003
Published: October 2, 2003

References

Abrieu, A., Brassac, T., Galas, S., Fisher, D., Labbe, J.C., and Doree, M. (1998). The Polo-like kinase Plx1 is a component of the MPF amplification loop at the G2/M-phase transition of the cell cycle in Xenopus eggs. J. Cell Sci. *111*, 1751–1757.

Bahassi el, M., Conn, C.W., Myer, D.L., Hennigan, R.F., McGowan, C.H., Sanchez, Y., and Stambrook, P.J. (2002). Mammalian Polo-like kinase 3 (Plk3) is a multifunctional protein involved in stress response pathways. Oncogene *21*, 6633–6640.

Carson, M. (1991). Ribbons 2.0. J. Appl. Crystallogr. *24*, 958–961.

Conn, C.W., Hennigan, R.F., Dai, W., Sanchez, Y., and Stambrook, P.J. (2000). Incomplete cytokinesis and induction of apoptosis by overexpression of the mammalian polo-like kinase, Plk3. Cancer Res. *60*, 6826–6831.

Descombes, P., and Nigg, E.A. (1998). The polo-like kinase Plx1 is required for M phase exit and destruction of mitotic regulators in Xenopus egg extracts. EMBO J. *17*, 1328–1335.

Durocher, D., Taylor, I.A., Sarbassova, D., Haire, L.F., Westcott, S.L., Jackson, S.P., Smerdon, S.J., and Yaffe, M.B. (2000). The molecular basis of FHA domain: phosphopeptide binding specificity and implications for phosphodependent signaling mechanisms. Mol. Cell *6*, 1169–1182.

Elez, R., Piiper, A., Giannini, C.D., Brendel, M., and Zeuzem, S. (2000). Polo-like kinase1, a new target for antisense tumor therapy. Biochem. Biophys. Res. Commun. *269*, 352–356.

Elia, A.E., Cantley, L.C., and Yaffe, M.B. (2003). Proteomic screen finds pSer/pThr-binding domain localizing Plk1 to mitotic substrates. Science *299*, 1228–1231.

Glover, D.M., Hagan, I.M., and Tavares, A.A. (1998). Polo-like kinases: a team that plays throughout mitosis. Genes Dev. *12*, 3777–3787.

Golan, A., Yudkovsky, Y., and Hershko, A. (2002). The cyclin-ubiquitin ligase activity of cyclosome/APC is jointly activated by protein kinases Cdk1-cyclin B and Plk. J. Biol. Chem. *277*, 15552–15557.

Golsteyn, R.M., Schultz, S.J., Bartek, J., Ziemiecki, A., Ried, T., and Nigg, E.A. (1994). Cell cycle analysis and chromosomal localization of human Plk1, a putative homologue of the mitotic kinases Drosophila polo and Saccharomyces cerevisiae Cdc5. J. Cell Sci. *107*, 1509–1517.

Grallert, A., and Hagan, I.M. (2002). Schizosaccharomyces pombe NIMA-related kinase, Fin1, regulates spindle formation and an affinity of Polo for the SPB. EMBO J. *21*, 3096–3107.

Hof, P., Pluskey, S., Dhe-Paganon, S., Eck, M.J., and Shoelson, S.E. (1998). Crystal structure of the tyrosine phosphatase SHP-2. Cell *92*, 441–450.

Izumi, T., and Maller, J.L. (1993). Elimination of cdc2 phosphorylation sites in the cdc25 phosphatase blocks initiation of M-phase. Mol. Biol. Cell *4*, 1337–1350.

Jang, Y.J., Lin, C.Y., Ma, S., and Erikson, R.L. (2002). Functional studies on the role of the C-terminal domain of mammalian polo-like kinase. Proc. Natl. Acad. Sci. USA *99*, 1984–1989.

Jones, T.A., Zou, J.Y., Cowan, S.W., and Kjeldgaard. (1991). Improved methods for binding protein models in electron density maps and the location of errors in these models. Acta Crystallogr. A *47*, 110–119.

Kumagai, A., and Dunphy, W.G. (1992). Regulation of the cdc25 protein during the cell cycle in Xenopus extracts. Cell *70*, 139–151.

Lane, H.A., and Nigg, E.A. (1996). Antibody microinjection reveals an essential role for human polo-like kinase 1 (Plk1) in the functional maturation of mitotic centrosomes. J. Cell Biol. *135*, 1701–1713.

Lee, K.S., and Erikson, R.L. (1997). Plk is a functional homolog of Saccharomyces cerevisiae Cdc5, and elevated Plk activity induces multiple septation structures. Mol. Cell. Biol. *17*, 3408–3417.

Lee, K.S., Yuan, Y.L., Kuriyama, R., and Erikson, R.L. (1995). Plk is an M-phase-specific protein kinase and interacts with a kinesin-like protein, CHO1/MKLP-1. Mol. Cell. Biol. *15*, 7143–7151.

Lee, K.S., Grenfell, T.Z., Yarm, F.R., and Erikson, R.L. (1998). Mutation of the polo-box disrupts localization and mitotic functions of the mammalian polo kinase Plk. Proc. Natl. Acad. Sci. USA *95*, 9301–9306.

Lee, K.S., Song, S., and Erikson, R.L. (1999). The polo-box-dependent induction of ectopic septal structures by a mammalian polo kinase, plk, in Saccharomyces cerevisiae. Proc. Natl. Acad. Sci. USA *96*, 14360–14365.

Leung, G.C., Hudson, J.W., Kozarova, A., Davidson, A., Dennis, J.W., and Sicheri, F. (2002). The Sak polo-box comprises a structural domain sufficient for mitotic subcellular localization. Nat. Struct. Biol. *9*, 719–724.

Liu, X., and Erikson, R.L. (2003). Polo-like kinase (Plk)1 depletion induces apoptosis in cancer cells. Proc. Natl. Acad. Sci. USA *100*, 5789–5794.

Liu, X., Brodeur, S.R., Gish, G., Songyang, Z., Cantley, L.C., Laudano, A.P., and Pawson, T. (1993). Regulation of c-Src tyrosine kinase activity by the Src SH2 domain. Oncogene *8*, 1119–1126.

Ma, S., Liu, M.A., Yuan, Y.L., and Erikson, R.L. (2003). The serum-inducible protein kinase Snk is a G(1) phase polo-like kinase that is inhibited by the calcium- and integrin-binding protein CIB. Mol. Cancer Res. *1*, 376–384.

May, K.M., Reynolds, N., Cullen, C.F., Yanagida, M., and Ohkura, H. (2002). Polo boxes and Cut23 (Apc8) mediate an interaction between polo kinase and the anaphase-promoting complex for fission yeast mitosis. J. Cell Biol. *156*, 23–28.

Moarefi, I., LaFevre-Bernt, M., Sicheri, F., Huse, M., Lee, C.H., Kuriyan, J., and Miller, W.T. (1997). Activation of the Src-family tyrosine kinase Hck by SH3 domain displacement. Nature *385*, 650–653.

Mundt, K.E., Golsteyn, R.M., Lane, H.A., and Nigg, E.A. (1997). On the regulation and function of human polo-like kinase 1 (PLK1):

effects of overexpression on cell cycle progression. Biochem. Biophys. Res. Commun. *239*, 377–385.

Nicholls, A., Sharp, K.A., and Honig, B. (1991). Protein folding and association: insights from the interfacial and thermodynamic properties of hydrocarbons. Proteins *11*, 281–296.

Nigg, E.A. (1998). Polo-like kinases: positive regulators of cell division from start to finish. Curr. Opin. Cell Biol. *10*, 776–783.

Orlicky, S., Tang, X., Willems, A., Tyers, M., and Sicheri, F. (2003). Structural basis for phosphodependent substrate selection and orientation by the SCFCdc4 ubiquitin ligase. Cell *112*, 243–256.

Otwinowski, Z., and Minor, W. (1997). Processing of X-ray diffraction data collected in oscillation mode. Meth. Enzymol. *276*, 307–326.

Reynolds, N., and Ohkura, H. (2003). Polo boxes form a single functional domain that mediates interactions with multiple proteins in fission yeast polo kinase. J. Cell Sci. *116*, 1377–1387.

Seong, Y.S., Kamijo, K., Lee, J.S., Fernandez, E., Kuriyama, R., Miki, T., and Lee, K.S. (2002). A spindle checkpoint arrest and a cytokinesis failure by the dominant-negative polo-box domain of Plk1 in U-2 OS cells. J. Biol. Chem. *277*, 32282–32293.

Sicheri, F., Moarefi, I., and Kuriyan, J. (1997). Crystal structure of the Src family tyrosine kinase Hck. Nature *385*, 602–609.

Smith, M.R., Wilson, M.L., Hamanaka, R., Chase, D., Kung, H., Longo, D.L., and Ferris, D.K. (1997). Malignant transformation of mammalian cells initiated by constitutive expression of the polo-like kinase. Biochem. Biophys. Res. Commun. *234*, 397–405.

Smits, V.A., Klompmaker, R., Arnaud, L., Rijksen, G., Nigg, E.A., and Medema, R.H. (2000). Polo-like kinase-1 is a target of the DNA damage checkpoint. Nat. Cell Biol. *2*, 672–676.

Sonnhammer, E.L., Eddy, S.R., Birney, E., Bateman, A., and Durbin, R. (1998). Pfam: multiple sequence alignments and HMM-profiles of protein domains. Nucleic Acids Res. *26*, 320–322.

Strausfeld, U., Fernandez, A., Capony, J.P., Girard, F., Lautredou, N., Derancourt, J., Labbe, J.C., and Lamb, N.J. (1994). Activation of p34cdc2 protein kinase by microinjection of human cdc25C into mammalian cells. Requirement for prior phosphorylation of cdc25C by p34cdc2 on sites phosphorylated at mitosis. J. Biol. Chem. *269*, 5989–6000.

Terwilliger, T.C., and Berendzen, J. (1999). Automated MAD and MIR structure solution. Acta Crystallogr. D Biol. Crystallogr. *55*, 849–861.

Toyoshima-Morimoto, F., Taniguchi, E., and Nishida, E. (2002). Plk1 promotes nuclear translocation of human Cdc25C during prophase. EMBO Rep. *3*, 341–348.

Verdecia, M.A., Bowman, M.E., Lu, K.P., Hunter, T., and Noel, J.P. (2000). Structural basis for phosphoserine-proline recognition by group IV WW domains. Nat. Struct. Biol. *7*, 639–643.

Xie, S., Wu, H., Wang, Q., Cogswell, J.P., Husain, I., Conn, C., Stambrook, P., Jhanwar-Uniyal, M., and Dai, W. (2001). Plk3 functionally links DNA damage to cell cycle arrest and apoptosis at least in part via the p53 pathway. J. Biol. Chem. *276*, 43305–43312.

Xie, S., Wu, H., Wang, Q., Kunicki, J., Thomas, R.O., Hollingsworth, R.E., Cogswell, J., and Dai, W. (2002). Genotoxic stress-induced activation of Plk3 is partly mediated by Chk2. Cell Cycle *1*, 424–429.

Xu, W., Harrison, S.C., and Eck, M.J. (1997). Three-dimensional structure of the tyrosine kinase c-Src. Nature *385*, 595–602.

Yaffe, M.B., and Cantley, L.C. (2000). Mapping specificity determinants for protein-protein association using protein fusions and random peptide libraries. Methods Enzymol. *328*, 157–170.

Yaffe, M.B., and Elia, A.E. (2001). Phosphoserine/threonine-binding domains. Curr. Opin. Cell Biol. *13*, 131–138.

Yaffe, M.B., and Smerdon, S.J. (2001). PhosphoSerine/threonine binding domains: you can't pSERious? Structure *9*, R33–R38.

Yaffe, M.B., Rittinger, K., Volinia, S., Caron, P.R., Aitken, A., Leffers, H., Gamblin, S.J., Smerdon, S.J., and Cantley, L.C. (1997). The structural basis for 14-3-3:phosphopeptide binding specificity. Cell *91*, 961–971.

Accession Numbers

Coordinates for the Plk1 PBD-phosphopeptide complex have been deposited in the Protein Data Bank under ID code 1UMW.